# Phosphorylation and Binding Interactions of CheY Studied by Use of Badan-Labeled Protein†

Richard C. Stewart* and Ricaele VanBruggen

*Department of Cell Biology & Molecular Genetics, University of Maryland, College Park, Maryland 20742*

*Received March 2, 2004; Revised Manuscript Received May 4, 2004*

ABSTRACT: In the chemotaxis signal transduction pathway of *Escherichia coli*, the response regulator protein CheY is phosphorylated by the receptor-coupled protein kinase CheA. Previous studies of CheY phosphorylation and CheY interactions with other proteins in the chemotaxis pathway have exploited the fluorescence properties of $Trp^{58}$, located immediately adjacent to the phosphorylation site of CheY ($Asp^{57}$). Such studies can be complicated by the intrinsic fluorescence and absorbance properties of CheA and other proteins of interest. To circumvent these difficulties, we generated a derivative of CheY carrying a covalently attached fluorescent label that serves as a sensitive reporter of phosphorylation and binding events and that absorbs and emits light at wavelengths well removed from potential interference by other proteins. This labeled version of CheY has the (dimethylamino)naphthalene fluorophore from Badan [6-bromoacetyl-2-(dimethylamino)naphthalene] attached to the thiol group of a cysteine introduced at position 17 of CheY by site-directed mutagenesis. Under phosphorylating conditions (or in the presence of beryllofluoride), the fluorescence emission of Badan-labeled $CheY^{M17C}$ exhibited an ∼10 nm blue shift and an ∼30% increase in signal intensity at 490 nm. The fluorescence of Badan-labeled $CheY^{M17C}$ also served as a sensitive reporter of CheY−CheA binding interactions, exhibiting an ∼50% increase in emission intensity in the presence of saturating levels of CheA. Compared to wild-type CheY, Badan-labeled CheY exhibited reduced ability to autodephosphorylate and could not interact productively with the phosphatase CheZ. However, with respect to autophosphorylation and interactions with CheA, Badan-CheY performed identically to wild-type CheY, allowing us to explore CheA-CheY phosphotransfer kinetics and binding kinetics without interference from the fluorescence/absorbance properties of CheA and ATP. These results provide insights into CheY interactions with CheA, CheZ, and other components of the chemotaxis signaling pathway.

*Escherichia coli*, *Salmonella typhimurium*, and numerous other motile bacteria modulate their swimming movements in response to the chemical composition of their immediate environments (*1*). This ability enables a swimming bacterium to migrate up gradients of beneficial chemicals (such as nutrients, which serve as attractants) and to migrate down gradients of noxious chemicals (such as phenol and some toxic metal ions, which serve as repellents) (*2*−*5*). The control of cell swimming pattern that underlies such chemotactic movements involves communication between cell surface chemoreceptor proteins and the flagellar motors that effect swimming movements and direction changes. This communication occurs quickly (within 50−200 ms of stimulus detection by the receptors) (*6*−*8*), and it involves rapid phosphorylation and dephosphorylation of a cytoplasmic signaling protein, CheY, that binds to the flagellar motors and modulates their rotational preferences (clockwise versus counterclockwise) (*9*, *10*). Phosphorylation of CheY is catalyzed by a receptor-coupled kinase, CheA, and dephosphorylation of P-CheY is catalyzed by CheZ (*11*, *12*). The relative rates of CheY phosphorylation and dephosphorylation are adjusted by the chemotaxis system in response to input from the chemotaxis receptors (*13*). For example, the response of the chemotaxis signaling network to chemorepellents (or to removal of attractants) is an increase in CheA autokinase activity, resulting in an increased level of phosphorylated CheY. When the chemoreceptors encounter attractant stimuli, they decrease CheA autokinase activity, and the level of phosphorylated CheY falls. This regulation of CheA autokinase activity occurs within the context of ternary complexes involving receptors, CheA, and CheW, an adapter that couples CheA to the receptors (*14*−*18*).

Electron microscopy studies (*18*) have provided glimpses of the overall architecture of signaling complexes generated in vitro, but the detailed structures of the macromolecular complexes have yet to be determined. High-resolution structural information is available for the individual components of the complex (CheA, CheW, and the receptor proteins) as well as for the downstream signaling proteins, CheY and CheB, that are phosphorylated by the signaling complex (*19*). For the work described here, an understanding of the 3-dimensional structures of CheA and CheY is extremely useful (Figures 1 and 2). CheY is a 126 amino acid, $\alpha/\beta$ protein in which five $\alpha$ helices surround a central five-strand $\beta$ sheet (Figure 1B) (*20*, *21*). $Asp^{57}$, the phosphorylation site (*22*), resides in the loop connecting $\beta 3$ to $\alpha 3$. Side chains of residues located in adjacent loops at this end of the CheY

† Supported by NIH Research Grant GM52853 to R.C.S.

* To whom correspondence should be addressed: phone 301-405-5475; fax 301-314-9489; e-mail rs224@umail.umd.edu.

10.1021/bi0495735 CCC: $27.50 
Published on Web 06/18/2004

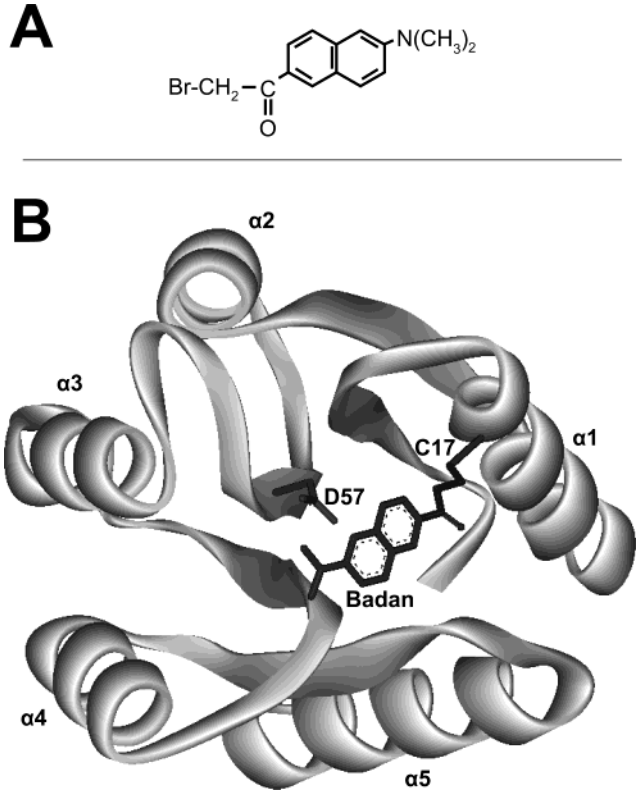


FIGURE 1: (A) Chemical structure of Badan and (B) three-dimensional structure of CheY. The ribbon diagram of the CheY structure was generated in Accelrys DS ViewerPro with coordinates from PDB file 1JBE (1.1 Å resolution) (*67*) that had been modified by changing Met[17] to Cys by use of the Mutate tool in Swiss PDBViewer DeepView V3.7 (*68*). Shown as dark gray stick models are the side chain of Asp[57] (the phosphorylation site), the side chain of Cys[17], and the acetyl(dimethylamino)naphthalene fluorophore group from Badan (attached to the thiol of Cys[17] and drawn to scale relative to the CheY structural elements by use of DS ViewerPro). In this view, the Asp[57] side chain is behind the Badan with the closest carboxylate oxygen of Asp[57] separated from the center of the naphthalene rings of the Badan by ~9 Å. The exact orientation of the fluorophore and the Cys side chain relative to the rest of CheY are hypothetical and were arrived at by minimizing (visually) steric clashes between the Cys-Badan and CheY side chains in the immediate vicinity. Numerous alternative orientations are possible. Computer-based energy minimization of the Badan-CheY was not attempted.

molecule comprise an active site that not only catalyzes phosphotransfer from CheA to CheY but also allows CheY to autophosphorylate in the presence of small-molecule phosphodonors such as acetyl phosphate and phosphoramidate (*23*, *24*).

Detailed structural information and a general understanding of the catalytic mechanism are also available for CheA. To achieve phosphorylation of CheY, CheA first autophosphorylates and then passes its phosphoryl group to CheY in a rapid phosphotransfer reaction (*11*). CheA has a modular organization, with distinct domains playing different roles in CheA's overall function (Figure 2). The P1 domain contains the phosphorylation site (His[48]) and presumably also encompasses features that interact with CheY to promote phosphotransfer (*25*). Domain P2 contains the binding site for CheY (*26*) and is connected to P1 by a flexible linker (*27*) such that CheY bound to P2 is tethered in close proximity to phosphorylated His[48], an arrangement that promotes CheA → CheY phosphotransfer kinetics (*28*).

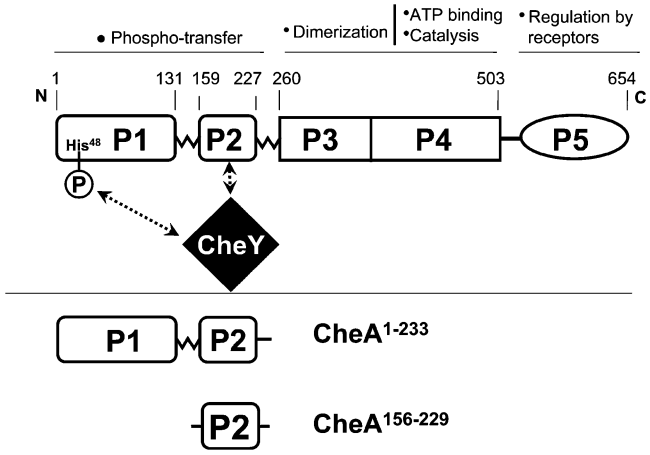


FIGURE 2: Schematic diagram of the structural and functional organization of CheA. The structures of domains P1−P5 have been characterized by a variety of approaches including NMR methods (*27*, *33*, *34*) and X-ray crystallography (*29*, *61*, *62*). CheA fragments used in this study included CheA$^{1-233}$ (which includes domains P1 and P2) and CheA$^{156-229}$ (P2 only). Functional roles for the various CheA domains have been deduced from the structural analyses as well as from proteolysis studies and analysis of selectively expressed protein fragments (*25*, *69*−*71*). These roles are discussed in the introduction.

Another flexible linker connects P2 to the domain (P3) that includes the helices responsible for CheA dimerization (*29*, *30*). Domain P4 contains the ATP-binding site and likely includes most of the kinase active-site determinants (*29*, *31*). The C-terminal domain P5 plays a key role in CheA regulation by binding to CheW and conveying regulatory signals from the receptor proteins to the CheA active site (*32*). Bilwes et al. (*29*) determined the structure of a CheA fragment spanning domains P3−P5 (i.e., domains P1 and P2 were absent). Detailed structural information is also available for domains P1 and P2 (*27*, *33*, *34*), but their orientation relative to P3−P5 has yet to be determined.

Experiments with purified preparations of CheY, CheA, and other components of the chemotaxis signaling pathway have made important contributions toward understanding how the signaling machinery of *E. coli* operates at a molecular level. For many such experiments, it is important to be able to monitor phosphorylation of CheY and its interactions with CheA. Such measurements are facilitated greatly by the location and fluorescence properties of the lone tryptophan residue of CheY. Trp[58] resides at the active site of CheY, immediately adjacent to the phosphorylation site (Asp[57]). The fluorescence emission intensity of Trp[58] decreases by ~50% upon phosphorylation, enabling fluorescence-based experiments to monitor CheY phosphorylation (*23*, *24*). CheY intrinsic fluorescence also decreases dramatically (*35*, *36*) as a consequence of CheY binding to either CheA or FliM, the docking site for CheY in the flagellar motor (*3*). The sensitivity of Trp[58] fluorescence to CheY phosphorylation and binding interactions has been a powerful tool, enabling investigations of the kinetics and biochemical mechanisms of the binding and phosphorylation reactions as well as providing a way to quantify the effects of various mutations on CheY activities (*24*, *37*−*41*). However, one limitation in using CheY intrinsic fluorescence as a signal for such experiments is that the other proteins of the chemotaxis signaling pathway (e.g., CheA) all have intrinsic fluorescence that that can interfere with or compli-

cate analysis of fluorescence-based experiments intended to observe CheY. Experiments requiring addition of other proteins and/or ATP to CheY samples are also complicated by the ability of these additions to absorb the UV light required for CheY fluorescence. To circumvent such problems, we have developed a variant of CheY that carries a fluorescent group (Badan)[1] that absorbs and emits light at longer wavelengths and that faithfully reports the phosphorylation status of CheY and its interactions with CheA. Figure 1A depicts the structure of Badan, and Figure 1B shows this structure in the context of the three-dimensional structure of Badan-labeled $CheY^{M17C}$.

## EXPERIMENTAL PROCEDURES

*Chemicals and Reagents.* TCEP [tris-(2-carboxyethyl)-phosphine], Badan [6-bromoacetyl-2-(dimethylamino)naphthalene], and all other thiol-reactive fluorophores were purchased from Molecular Probes. Beryllium chloride, sodium fluoride, and acetyl phosphate (the lithium, potassium salt) were purchased from Aldrich Chemical Co. TNKGDG buffer contained 50 mM Tris-HCl, 50 mM potassium glutamate, 25 mM NaCl, 0.5 mM DTT, and 10% glycerol (v/v) adjusted to pH 7.5 at 25 °C.

*Site-Directed Mutants, Plasmids, and Bacterial Strains.* Cysteine substitution mutations were introduced into *cheY* by oligonucleotide-directed mutagenesis as described by Kunkel et al. (*42*). Mutations created unique silent restriction sites and were confirmed by DNA sequencing. The template DNA for the mutagenesis was pTZ18U:cheY, a plasmid that carries *E. coli cheY* on a 390-bp *Nde*I−*Xba*I insert. The *Nde*I and *Xba*I sites flanking *cheY* were introduced in the PCR primers used to amplify *cheY* during creation of pTZ18U:cheY. For high-level production of CheY protein, *cheY* was inserted into plasmid pET28a (Novagen). To assess the ability of $CheY^{M17C}$ and other mutant CheY proteins to support chemotaxis, the corresponding *cheY* alleles were inserted into plasmid pAR1:cheY (*43*) and transformed into Δ*cheY* strain D152recA. Transformants were stabbed into trpytone swarm plates (*44*), and swarming ability was measured relative to that of D152recA transformants carrying pAR1:cheYwildtype and pAR1 lacking *cheY*. Measurements of swarming rates were made as described by Smith et al. (*45*). pAR1:cheY is a derivative of pCW (*46*); it has *cheY* located downstream of a hybrid *lac*−*tac* promoter (*47*) and carries $lacI^q$, enabling IPTG-regulated expression of *cheY* over a wide range spanning that observed in wild-type cells. *E. coli* strain D152recA was created by P1 transduction of *recA1 srl*::Tn*10* into strain RP5221 (*cheY*Δm60−21) (*48*).

*Protein Preparations.* CheY, $CheY^{M17C}$, and other variants of CheY carrying cysteine substitutions were overproduced in *E. coli* host cells BL21 λDE3 (*49*) by use of expression plasmid pET28a:cheY. This plasmid directed production of CheY carrying an N-terminal $(His)_6$ affinity tag that was exploited during the first step of the protein purification: Ni−NTA affinity chromatography was performed on soluble, cytoplasmic extracts of BL21/pET28a:cheY generated by sonication followed by ultracentrifugation. The buffers, loading, washing, and elution protocols were as described previously by Levit et al. (*50*), except that 1 mM β-mercaptoethanol was included in all buffers to maintain the reduced state of the cysteines introduced into CheY. CheY fractions eluted from the Ni−NTA column were pooled, dialyzed into TEDG buffer [50 mM Tris, 0.5 mM $Na_2EDTA$, 0.5 mM DTT, and 10% (v/v) glycerol], and then further purified by chromatography on DEAE-Sepharose as described previously (*51*).

$(His)_6$-CheA was purified from BL21 λDE3/pET14b:cheA by following published methods (*52*). CheA fragments [$(His)_6$-$CheA^{1-139}$, $(His)_6$-$CheA^{156-229}$, and $(His)_6$-$CheA^{1-233}$] were purified from cytoplasmic extracts of BL21 λDE3 carrying the appropriate pET overexpression vector (pET14b:P1, pET14b:P2, and pET14b:P1P2, respectively). This involved use of a Ni−NTA column as described by Levit et al. (*50*) followed by a DEAE-Sephacel column.

For CheA and CheY samples, protein concentrations were determined spectrophotometrically by use of calculated extinction coefficients [8.25 $mM^{-1}$ $cm^{-1}$ for CheY and 16.3 $mM^{-1}$ $cm^{-1}$ for CheA] (*53*). For $(His)_6$-$CheA^{1-139}$, $(His)_6$-$CheA^{156-229}$, and $(His)_6$-$CheA^{1-233}$, protein concentrations were determined with the BCA assay kit from Pierce Chemical Co. (with bovine serum albumin as the standard). His-tagged proteins carried an N-terminal extension of MGSSHHHHHHSSGLVPRGSH. This additional sequence does not appear to affect the activities of CheA (*52*, *54*) and CheY [R.C.S., unpublished observations] either in vitro or in vivo, and so we did not remove the His tag from our purified protein preparations before using them for experiments. For convenience, we do not explicitly indicate the presence of the His tag in the names of the proteins in the Results, Discussion, and the remainder of Experimental Procedures.

*Labeling $CheY^{M17C}$ with Badan.* $CheY^{M17C}$ protein was stored in buffer containing 0.5 mM DTT, which would readily react with the thiol-reactive Badan and prevent labeling of the protein. To remove the DTT yet maintain the reduced state of the CheY cysteine side chain, we dialyzed $CheY^{M17C}$ samples extensively against 50 mM Tris and 0.5 mM EDTA containing 1 mM TCEP. To a 100 μM $CheY^{M17C}$ dialyzed sample (100 μL), small aliquots (5 × 2 μL) were added from a 25 mM Badan stock solution (prepared by dissolving Badan in dimethylformamide). The protein sample was mixed continuously during addition of the fluorescent label. The labeling reaction was allowed to proceed in the dark for 2 h at room temperature. Then β-mercaptoethanol was added to quench the reaction (5 mM final concentration), and the sample was dialyzed extensively against TED buffer at 4 °C in the dark (8 × 500 mL). The stoichiometry of labeling was quantified as described by Boxrud et al. (*55*). This involved measuring the absorbance spectrum of labeled protein in a denaturing buffer (6 M guanidine hydrochloride, 0.1 M Tris-HCl, and 1 mM EDTA, pH 8.5) and determining the protein concentration by use of the micro-bicinchoninic acid assay from Pierce Chemical Co. (with wild-type CheY as the standard). The concentration of Badan in the labeled sample was calculated with an extinction coefficient of 12.9 $mM^{-1}$ $cm^{-1}$ for thiol-linked Badan at 387 nm (*55*). Samples

[1] Abbreviations: Badan, 6-bromoacetyl-2-(dimethylamino)naphthalene; DMF, *N*,*N*-dimethylformamide; DMSO, dimethyl sulfoxide; TCEP, tris(2-carboxyethyl)phosphine; P-CheY, phosphorylated CheY; P-CheA, phosphorylated CheA; DTT, dithiothreitol; IPTG, isopropyl β-thiogalactoside; PCR, polymerase chain reaction; NTA, nitrilotriacetate; EDTA, ethylenediaminetetraacetate; DEAE, diethylaminoethyl; BCA, bicinchoninic acid; SDS−PAGE, sodium dodecyl sulfate−polyacrylamide gel electrophoresis.

from three independent labeling experiments gave stoichiometries between 0.88 and 1.13.

*Fluorescence-Monitored Binding and Phosphorylation Titrations.* Fluorescence excitation and emission spectra were recorded on a PTI QuantaMaster instrument. Samples (2.5 mL) were placed in standard 1 cm × 1 cm quartz cuvettes, maintained at 25 °C in a thermostated cuvette holder, and subjected to continuous stirring with a magnetic stir bar. To monitor the intrinsic fluorescence of wild-type CheY, emission spectra were recorded by scanning from 290 to 440 nm (emission slits set at 5 nm) with an excitation wavelength of 284 nm (excitation slits set at 1.5 nm). To monitor emission of the (dimethylamino)naphthalene fluorophore of Badan-CheY, an excitation wavelength of 390 nm was used (1.5 nm excitation slits), and emission spectra were recorded from 400 to 600 nm (emission slits set at 5 nm). Binding data from fluorescence-monitored titrations were analyzed by least-squares fitting routines in Dynafit (*56*) or SigmaPlot (assuming a simple one-site binding model). Results were corrected for the effects of dilution prior to such analysis. Titration experiments were performed in TNKGDG buffer.

*Rapid Reaction Measurements.* Stopped-flow fluorescence measurements were performed on an Applied Photophysics SX-17MV instrument. The wavelength of the excitation light (284 nm for CheY intrinsic fluorescence, 390 nm for Badan-CheY) was controlled by a monochromator. Emission intensities were monitored with a photomultiplier after passing through a second monochromator or, for some experiments, after passing through a long-pass filter (WG320 for CheY intrinsic fluorescence; OG420 for Badan-CheY). These two instrument configurations gave equivalent results. The dead time of the instrument was determined to be 0.8 ms by the Massey procedure (*57*). In a typical experiment, ~50 $\mu$L of CheY (or Badan-CheY) was rapidly mixed with an equal volume of a second solution (containing CheA or acetyl phosphate, for example), and the ensuing changes in emission signal were monitored over an appropriate time scale. Time courses from 10 consecutive shots (each containing 2000 data points) were averaged and then analyzed with the Applied Photophysics software. Experiments were performed in TNKGDG buffer, and the temperature was regulated in a circulating water bath (25 °C for CheY phosphorylation/dephosphorylation experiments; 4 °C for CheY−CheA binding experiments).

*Additional CheY Cysteine-Substitution Mutants and Fluorophores.* In addition to $CheY^{M17C}$, we purified and fluorescently labeled the following CheY variants: N23C, M63C, D64C, V87C, A88C, V107C, and T112C. Each CheY variant was labeled with Acrylodan [6-acryloyl-2-(dimethylamino)-naphthalene], Badan [6-bromoacetyl-2-(dimethylamino)-naphthalene], DCIA [7-diethylamino-3-((4′- (iodoacetyl)-amino)phenyl)-4-methylcoumarin], IAEDANS [5-((((2-iodoacetyl)amino)ethyl)amino)naphthalene-1-sulfononic acid], Oregon Green 488 maleimide, and AlexaFluor594 maleimide. The procedures for covalent attachment of the fluorophores to CheY were as described above for Badan labeling of $CheY^{M17C}$, except that in some instances the stock solution of the thiol-reactive compound was prepared in DMSO instead of DMF. Each labeled CheY sample was examined for phosphorylation-dependent fluorescence changes by recording emission spectra in the absence and presence of 10 mM acetyl phosphate and 10 mM $MgCl_2$.

## RESULTS

*Screening CheY Cysteine-Substitution Mutants and Fluorophores.* Our initial goal was to generate a fluorescently labeled derivative of CheY that, upon phosphorylation, exhibited an easily monitored change in fluorescence emission at wavelengths where absorbance and emission properties of unlabeled proteins and ATP would not interfere. To attach a variety of fluorophores to CheY at different selected locations, we used thiol-reactive fluorescent molecules that formed covalent attachments to cysteine side chains that we had introduced into CheY. Wild-type CheY (from *E. coli*) lacks cysteine; we used oligonucleotide-directed mutagenesis to introduce single cysteine substitutions at eight distinct positions in the protein ($Met^{17}$, $Asn^{23}$, $Met^{63}$, $Asp^{64}$, $Val^{87}$, $Ala^{88}$, $Val^{107}$, and $Thr^{112}$). These substitution sites were chosen because they (i) were located at positions that, on the basis of previous NMR and crystallography studies, undergo changes in position/environment upon phosphorylation of CheY (*58*−*60*); (ii) were situated on the surface of the protein, in helices or loops, and seemed capable of accommodating an amino acid substitution and attachment of a relatively bulky fluorophore without disrupting the overall conformation of the protein; and (iii) were not expected to alter CheY side chains directly involved in formation of the CheY−CheA or CheY−FliM complexes (*61*−*63*). We did not consider possible effects of mutations on CheY interactions with CheZ because we initiated these studies before the structure of the CheY−CheZ complex was defined (*64*). For each of the eight cysteine-substitution mutants, seven different thiol-reactive fluorophores were covalently attached, and then the fluorescence emission properties of the labeled proteins were examined in the absence and presence of $Mg^{2+}$ and acetyl phosphate, a small molecule phosphodonor that can readily phosphorylate CheY (*23*). The specific fluorophores that we used are described under Experimental Procedures. Of 56 different mutant−fluorophore combinations, only one, $CheY^{M17C}$ labeled with Badan, gave rise to a relatively large change in fluorescence emission under phosphorylating conditions. The details of this spectral change are presented below. The other six fluorophores attached at position 17 of $CheY^{M17C}$ were not changed by phosphorylating conditions. This was particularly surprising for the Acrylodan-labeled protein: the fluorophore of Acrylodan is identical to that of Badan, and the only difference in the labeled proteins would be one methylene ($-CH_2$) group in the short chain linking the cysteine sulfhydryl to the naphthalene rings of the fluorophore. The insensitivity of Acrylodan-$CheY^{M17C}$ fluorescence to phosphorylation and the lack of success we encountered with 55 of the 56 protein−fluorophore combinations underscore some of the difficulties associated with creating fluorescent reporter derivatives that function in the intended manner, even when detailed information is available about the structure of the protein being labeled.

*Labeling of $CheY^{M17C}$ and Fluorescence Properties of Badan-CheY.* Treatment of $CheY^{M17C}$ with Badan resulted in extensive covalent attachment of the fluorescent label to CheY: SDS−PAGE analysis of labeled CheY samples (after extensive dialysis) indicated the presence of a single fluorescent band at the gel position corresponding to CheY (as indicated by Coomassie staining, results not shown).

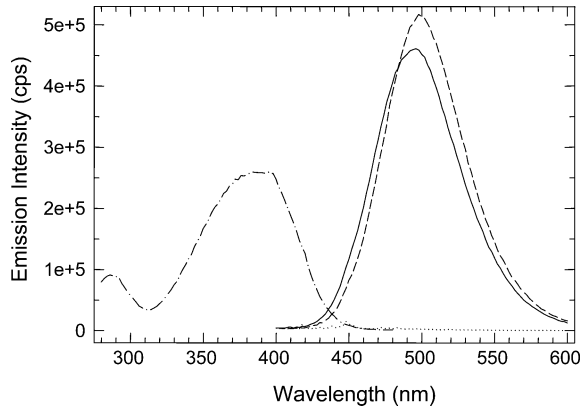


FIGURE 3: Fluorescence spectra of Badan-CheY. Emission spectra were recorded ($\lambda_{ex}$ 390 nm) for 0.25 $\mu$M Badan-CheY in TNGKGD buffer in the absence (—) or presence (− − −) of 10 mM $MgCl_2$ at 25 °C. The excitation spectrum (− · −) was recorded for the same protein sample (in the absence of $MgCl_2$) with $\lambda_{em}$ = 495 nm.

Importantly, this labeling was not observed with wild-type CheY (which lacks cysteine), and no fluorescent material was observed at the dye front of such gels, suggesting that all of the Badan present in labeled $CheY^{M17C}$ samples was covalently attached to the protein (i.e., dialysis was effective in removing unattached Badan). In three separate labeling experiments, the stoichiometry of the modification was 0.83−1.13 Badan molecules per $CheY^{M17C}$ molecule, based on the absorbance spectrum of the final labeled product and the protein concentration. This stoichiometry calculation is detailed under Experimental Procedures.

Figure 3 shows the excitation and emission spectra of the Badan-labeled $CheY^{M17C}$, which we will refer to as Badan-CheY for the remainder of this paper. Addition of $Mg^{2+}$ to Badan-CheY altered the emission spectrum of the protein. This effect was reversed upon addition of excess EDTA (results not shown). $Mg^{2+}$ is known to bind to the CheY active site, forming a complex in which three of the six sites of the $Mg^{2+}$ coordination sphere are contributed by CheY residues (carboxylate oxygens from $Asp^{13}$ and $Asp^{57}$ and the carbonyl oxygen of $Asn^{59}$) (*21*). In this complex, the fluorescence emission of $Trp^{58}$ is diminished (*65*). Our results suggest that binding of $Mg^{2+}$ to the CheY active site alters the environment of the fluorophore in Badan-CheY.

We observed a distinct and more dramatic change in the Badan emission spectrum upon addition of small molecule phosphodonors such as acetyl phosphate (Figure 4A) and phosphoramidate (data not shown) to Badan-CheY in the presence of $Mg^{2+}$. This fluorescence change was not observed in the absence of $Mg^{2+}$ or when excess EDTA was added to Badan-CheY + $Mg^{2+}$ solutions prior to addition of acetyl phosphate (results not shown). Similar spectral changes were also observed when ATP was added to a mixture of CheA and Badan-CheY, but again only in the presence of $Mg^{2+}$ (results not shown).

As shown in Figure 4B, a similar increase in fluorescence emission intensity was observed when $BeCl_2$ was added to a Badan-CheY solution containing NaF, conditions previously demonstrated to generate beryllofluoride ($BeF_3^-$), an anion capable of binding to the active site of CheY (and other response regulator proteins) in a manner that mimics acyl-phosphate formation at $Asp^{57}$: i.e., binding of $BeF_3^-$

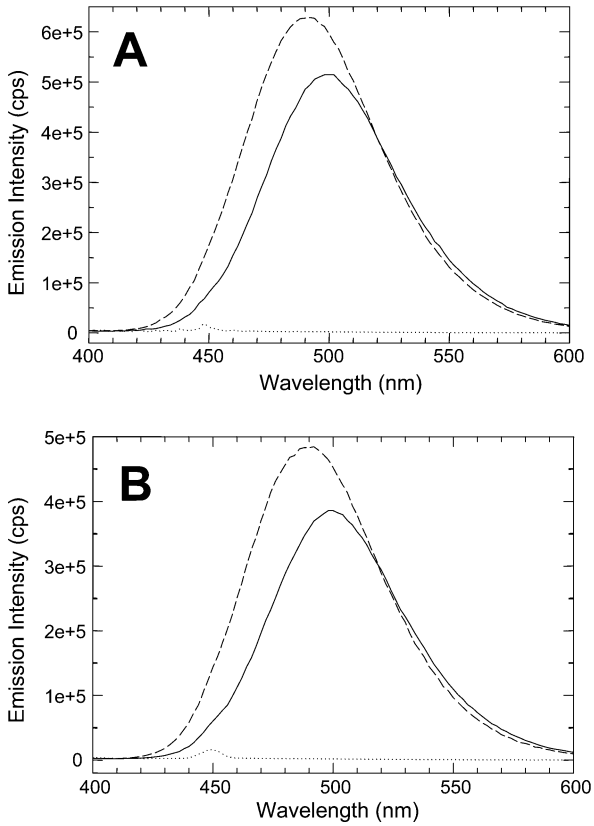


FIGURE 4: Effect of phosphorylation and beryllofluoride on fluorescence emission of Badan-CheY. Spectra were recorded for Badan-CheY samples at 25 °C with $\lambda_{ex}$ = 390 nm. (A) Badan-CheY (0.25 $\mu$M) in the absence (—) or presence (− − −) of 10 mM acetyl phosphate (both in the presence of 10 mM $MgCl_2$). (B) Badan-CheY (0.20 $\mu$M) in buffer containing 10 mM NaF and 10 mM $MgCl_2$ in the absence (—) or presence (− − −) of 200 $\mu$M $BeCl_2$. The dotted line in each panel shows the emission spectrum observed for a buffer blank prior to addition of the Badan-CheY. Spectra have been corrected for a small dilution effect caused by the addition of acetyl phosphate or $BeCl_2$.

to CheY forms a stable complex in which the protein adopts an activated conformation that closely resembles the conformation of phosphorylated CheY (*59*, *66*). The Badan-CheY spectral change caused by $BeF_3^-$ was observed in the presence of $MgCl_2$ but not in its absence, as expected given previous observations that a divalent metal ion is required for formation of the $BeF_3^-$ complex with CheY and other response regulator proteins (*66*).

The results in Figure 4 indicate that phosphorylation of Badan-CheY gives rise to a 10 nm blue shift in the $\lambda_{max}$ of Badan emission and approximately a 30% increase in the emission intensity at 490 nm. The fluorophore of Badan is a (dimethylamino)naphthalene group (Figure 1A). Figure 1B shows the location of the $Met^{17}$ side chain in the 3-dimensional structure of CheY and indicates that a fluorophore attached to a side chain at position 17 could be oriented adjacent to the phosphorylation site ($Asp^{57}$). It is possible that the electronic environment of the fluorophore is altered directly by CheY phosphorylation and $BeF_3^-$. Alternatively, the observed emission change could reflect the altered conformation of the protein caused by phosphorylation (*58*−*60*).

*Fluorescence-Monitored Phosphorylation and Dephosphorylation Kinetics of Badan-CheY.* We performed stopped-flow fluorescence experiments to determine (i) the kinetics

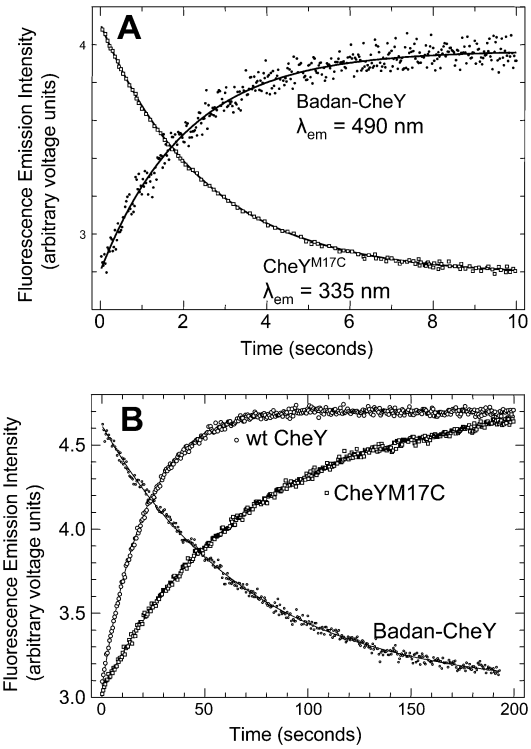


FIGURE 5: Kinetics of autophosphorylation and autodephosphorylation for wild-type CheY, CheY$^{M17C}$, and Badan-CheY. (A) Fluorescence stopped-flow measurements of emission intensity (at the indicated wavelengths) were made after CheY was mixed with 100 mM acetyl phosphate in TNGKGD buffer at 25 °C. Badan-CheY (1 $\mu$M) and unlabeled CheY (wild-type and CheY$^{M17C}$, 10 $\mu$M) were used (concentrations are those in the observation cell after mixing). Results obtained with wild-type CheY (not shown) were identical to those reported for CheY$^{M17C}$. First-order analysis of the time courses indicated $k_{obs}$ values of 0.38 $s^{-1}$ for Badan-CheY, 0.4 $s^{-1}$ for CheY$^{M17C}$, and 0.39 $s^{-1}$ for wild-type CheY. (B) Results of pH-jump experiments to monitor CheY dephosphorylation kinetics as described previously (*39*, *72*). A solution containing CheY (2 $\mu$M Badan-CheY, 20 $\mu$M CheYM17C, or 20 $\mu$M wild-type CheY) and 50 mM potassium phosphoramidate was generated in dilute buffer (5 mM Tris and 10 mM $MgCl_2$, pH 7.0) and then introduced into one drive syringe of the stopped-flow instrument. Concentrated, high-pH buffer (0.2 M CAPS, pH 10.5, containing 10 mM $MgCl_2$ and 50 mM potassium phosphoramidate) was placed in the second drive syringe. Small amounts of the solutions in the drive syringes (50 $\mu$L at a time) were then mixed rapidly (1:1) and delivered to the observation cell. The ensuing fluorescence changes were monitored and analyzed, indicating first-order rate constants of 0.045 $s^{-1}$ for autodephosphorylation of wild-type CheY and 0.014 $s^{-1}$ for both Badan-CheY and CheY$^{M17C}$.

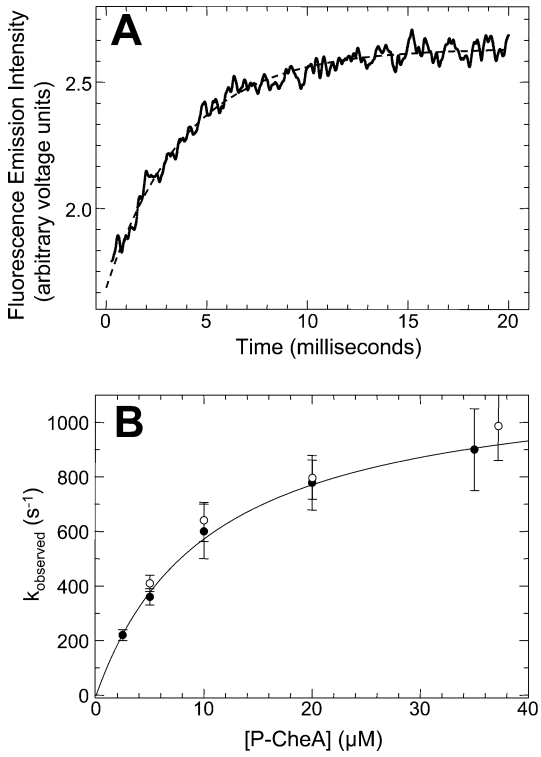


FIGURE 6: Kinetics of phosphotransfer from P-CheA to Badan-CheY. (A) Stopped-flow fluorescence measurements were used to monitor the reaction between 0.25 $\mu$M Badan CheY and 2.5 $\mu$M P-CheA at 25 °C with $\lambda_{ex}$ = 390 nm. Emission intensity at wavelengths greater than 420 nm was observed by use of a long-pass filter (OG420) between the observation cell and the photomultiplier. The data (—) are fit well by a single-exponential time course (– – –), indicating $k_{obs}$ = 220 ± 5 $s^{-1}$. (B) Analysis of the effect of P-CheA concentration on the rate of the phosphotransfer reaction, monitored as in panel A. Data sets are shown for two different ways of generating phosphorylated CheA. For one data set (●), P-CheA was generated by incubating CheA with 10 mM ATP (and $MgCl_2$) and then removing the excess ATP (and ADP) by column chromatography as described previously (*11*). For the second data set (○), P-CheA was generated in the loading syringe of the stopped-flow instrument by adding 10 mM ATP to the CheA sample immediately before use. This CheA + ATP + $MgCl_2$ mixture was then used directly without prior removal of the ATP. The two data sets gave equivalent results. The solid line depicts the results of least-squares fitting of the ● data set by use of a simple rectangular hyperbolic function and indicates a $K_m$ of 10.5 ± 1.2 $\mu$M and $k_{cat}$ of 1000 ± 200 $s^{-1}$. Fitting the ○ data set gave comparable values for $K_m$ and $k_{cat}$.

of Badan-CheY autophosphorylation in the presence of acetyl phosphate, (ii) the kinetics of autodephosphorylation of Badan-CheY-P, and (iii) the kinetics of phosphotransfer from P-CheA to Badan-CheY. To assess individually the effects of the Badan label and the Met$^{17}$ → Cys substitution on the properties of CheY, we also conducted similar experiments using unlabeled CheY$^{M17C}$ and wild-type CheY. The rate of autophosphorylation of Badan-CheY was determined by monitoring the fluorescence emission after rapid mixing of the fluorescently labeled protein with acetyl phosphate. At each of a series of concentrations of acetyl phosphate, this fluorescence increase was fit well by a single-exponential equation (Figure 5A). Similar experiments were performed with unlabeled CheY$^{M17C}$ (Figure 5A) and wild-type CheY (results not shown) by monitoring the decrease in intrinsic fluorescence (of Trp$^{58}$) resulting from autophosphorylation. The rate of autophosphorylation of Badan-CheY was essentially the same as that observed with unlabeled CheY$^{M17C}$ and wild-type CheY.

We also investigated the kinetics of Badan-CheY phosphorylation by P-CheA. To monitor this rapid reaction, we used stopped-flow fluorescence experiments to observe the emission change after a limiting concentration of Badan-CheY was mixed with excess P-CheA at a series of concentrations (Figure 6A). Each time course was fit well to a single-exponential equation to extract an observed pseudo-first-order rate constant ($k_{obs}$). The hyperbolic dependence of $k_{obs}$ on P-CheA concentration (Figure 6B) indicated a $K_m$ value of ~10 $\mu$M and a limiting rate constant of phosphotransfer (extrapolated to infinite P-CheA concentration) of ~1000 $s^{-1}$. These results are comparable to those obtained previously with wild-type CheY by monitoring the decrease in CheY intrinsic fluorescence (Trp$^{58}$) [$k_{cat}$ = 800 ± 200

$s^{-1}$; $K_m = 7 \pm 2$ $\mu$M] (*39*). Moreover, these experiments illustrate how using Badan-CheY provides some advantages over employing the intrinsic fluorescence of wild-type CheY as a way to monitor CheY phosphorylation status. In our previous studies (*39*), the strong fluorescence emission signal of CheA dictated that we perform the phosphotransfer experiments with CheY in excess over a limiting amount of P-CheA, and the highest CheY concentration that provided useful information was ~20 $\mu$M; higher levels of CheY gave rise to unacceptable signal-to-noise ratios because of the high starting fluorescence of the CheY. Using Badan-CheY, we were able to significantly extend these earlier studies by using P-CheA in excess over CheY and by working with close-to-saturating levels of P-CheA (up to 100 $\mu$M). In addition, the Badan-CheY experiments allowed us to include millimolar levels of ATP in the reaction mixture to ensure maximal phosphorylation of CheA, as detailed in the caption for Figure 6. Such an addition is problematic in experiments that rely on CheY intrinsic fluorescence because absorbance of the excitation light by the ATP decreases the $Trp^{58}$ emission signal. The results presented above indicate that the (dimethylamino)naphthalene fluorophore and $Met^{17} \rightarrow$ Cys substitution of Badan-CheY do not affect CheY phosphorylation or its interactions with CheA.

To monitor the kinetics of CheY dephosphorylation, we performed pH-jump experiments in which preequilibrated mixtures of CheY and phosphoramidate were subjected to a rapid pH increase that served to stop subsequent rounds of CheY autophosphorylation (*39*). The pH-insensitive autodephosphorylation reaction (*24*) then gave rise to fluorescence changes over the subsequent 200 s (Figure 5B). Each fluorescence time course was fit well by a single-exponential equation. These experiments indicated that Badan-CheY and $CheY^{M17C}$ catalyzed autodephosphorylation at about 30% of the rate observed with wild-type CheY.

We also investigated the influence of the $Met^{17} \rightarrow$ Cys substitution and attachment of the Badan label on the ability of CheY to interact productively with CheZ. CheZ catalyzes dephosphorylation of P-CheY (*11*, *12*). This ability can be visualized easily by adding substoichiometric amounts of CheZ to mixtures of CheY and acetyl phosphate (Figure 7) (*23*). In such a mixture, the steady-state level of phosphorylation of CheY (as indicated by its fluorescence) reflects the relative rates of autophosphorylation and dephosphorylation. As sequential additions of CheZ are made to the mixture, the steady-state level of phosphorylated CheY decreases in a progressive manner (i.e., the intrinsic fluorescence of wild-type CheY increases). With wild-type CheY (at 10 $\mu$M) and 0.25 mM acetyl phosphate, a CheZ concentration of 0.02 $\mu$M was sufficient to decrease the P-CheY steady level by 50%, and a concentration of 0.1 $\mu$M CheZ reduced the level of phosphorylated CheY to undetectable levels. With unlabeled $CheY^{M17C}$ (10 $\mu$M), CheZ had a qualitatively similar effect but higher concentrations of CheZ were required to accomplish comparable levels of dephosphorylation. With Badan-CheY, CheZ additions were completely ineffective in reversing the phosphorylation-induced fluorescence change. We conclude that the $Met^{17} \rightarrow$ Cys substitution has a modest effect on CheY−CheZ interactions and that addition of the bulky (dimethylamino)naphthalene group at position 17 drastically reduces or even eliminates productive interaction between CheY and CheZ. This loss of sensitivity to CheZ could reflect either loss of binding or disruption of catalytic events after binding of CheZ to P-CheY.

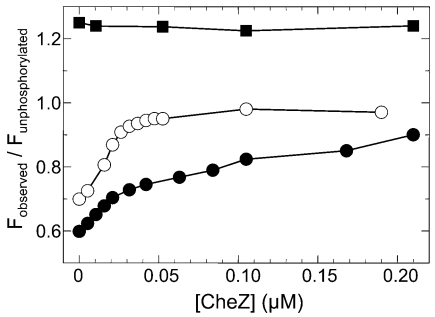


FIGURE 7: Effectiveness of CheZ in catalyzing dephosphorylation of wild-type CheY(○), $CheY^{M17C}$ (●), and Badan-CheY (■). To begin each experiment, a fluorescence emission spectrum was recorded for the CheY sample ($\lambda_{ex} = 390$ nm for Badan-CheY; $\lambda_{ex} = 284$ nm for wild-type CheY and $CheY^{M17C}$) in buffer containing 10 mM $MgCl_2$. Then acetyl phosphate was added (final concentration 0.25 mM) to generate a steady-state mixture of phosphorylated and unphosphorylated CheY. The emission spectrum of this mixture was recorded and used to calculate the starting ratio of $F_{observed}/F_{unphosphorylated}$. Then successive additions of CheZ were made, and emission spectra were recorded after each addition. The fluorescence changes resulting from CheZ addition reflect an adjustment of the steady-state concentration of P-CheY as the dephosphorylation rate is increased by progressively higher CheZ concentrations until a point is reached (at the highest CheZ concentrations) where the steady-state P-CheY level is undetectable. The $CheY^{M17C}$ and wild-type CheY results shown in the figure were corrected for a small level of CheZ intrinsic fluorescence (less than 5% of the observed signal change at the highest CheZ concentration). Wild-type CheY and $CheY^{M17C}$ were used at 10 $\mu$M, and emission intensities at 340 nm were monitored. Badan-CheY was used at 0.5 $\mu$M, and emission intensities at 490 nm were analyzed to monitor its phosphorylation status. Lines connecting the data points are included for clarity and are not based on any calculations or model.

*Effects of CheA Binding on Badan-CheY Fluorescence.* CheY binds rapidly to CheA, forming a complex with $K_d \sim 1$ $\mu$M. With micromolar concentrations of wild-type CheY and CheA, the association reaction is complete within ~50 ms even at 4 °C in the presence of viscogens such as glycerol that slow the diffusion-limited binding reaction (*38*). This association involves CheY interacting with a binding site located in the P2 domain of CheA, and the affinity of CheY for the isolated P2 domain is approximately the same as that for the full-length CheA protein (*26*). Formation of the CheY−CheA complex results in a significant decrease (by ~30%) in the intrinsic fluorescence emission intensity of CheY, apparently reflecting alteration of the environment of $Trp^{58}$ at the CheY active site (*35*, *37*, *38*). We investigated the effect of CheA on the fluorescence properties of Badan-CheY. As shown in Figure 8A, addition of full-length CheA to Badan-CheY gave rise to a large increase in the emission intensity of the dimethylaminonaphthalene fluorophore of the labeled CheY. We observed a very similar change in fluorescence emission spectrum when saturating levels of a CheA fragment ($CheA^{1-233}$) spanning domains P1 and P2 were added, but not when we added saturating levels of the P2 domain alone ($CheA^{156-229}$). We analyzed the results of titration experiments in which we monitored the emission intensity of Badan-CheY following successive additions of $CheA^{1-233}$ in the presence and absence of $CheA^{156-229}$ (Figure 8B). These binding curves indicated a $K_d$ of 1.8 ± 0.2 $\mu$M for the Badan-CheY−$CheA^{1-233}$ complex in the absence of

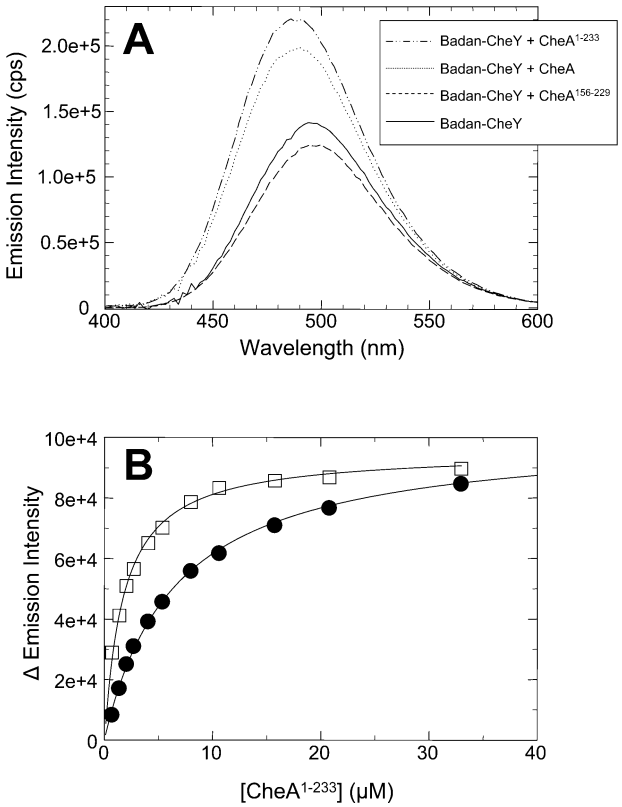


FIGURE 8: Effect of CheA binding on fluorescence emission of Badan-CheY. (A) Emission spectra were recorded for Badan-CheY samples (0.11 $\mu$M) in TNKGDG buffer (no $MgCl_2$) at 25 °C in the absence of CheA (—), in the presence of 20 $\mu$M $CheA^{156-229}$ (– – –), in the presence of 20 $\mu$M full-length wild-type CheA (· ··), or in the presence of 20 $\mu$M $CheA^{1-233}$ (– ·· –). (B) Results of fluorescence-monitored titration of Badan-CheY with $CheA^{1-233}$ in the absence (□) or presence (●) of 4.5 $\mu$M $CheA^{156-229}$. The change in emission intensity at 490 nm (plotted on the *y*-axis of this graph) was determined after each of a series of $CheA^{1-233}$ additions to a 0.1 $\mu$M Badan-CheY sample. The solid lines on this plot show the computer-generated best fits of the data to a simple, one-site binding equation. This analysis indicated a $K_d$ of 1.8 ± 0.1 $\mu$M for the Badan-CheY−$CheA^{1-233}$ complex and an apparent $K_d$ of 6.5 ± 0.2 $\mu$M in the presence of 4.5 $\mu$M $CheA^{156-229}$, reflecting competition between P2 and P1−P2 for Badan-CheY.

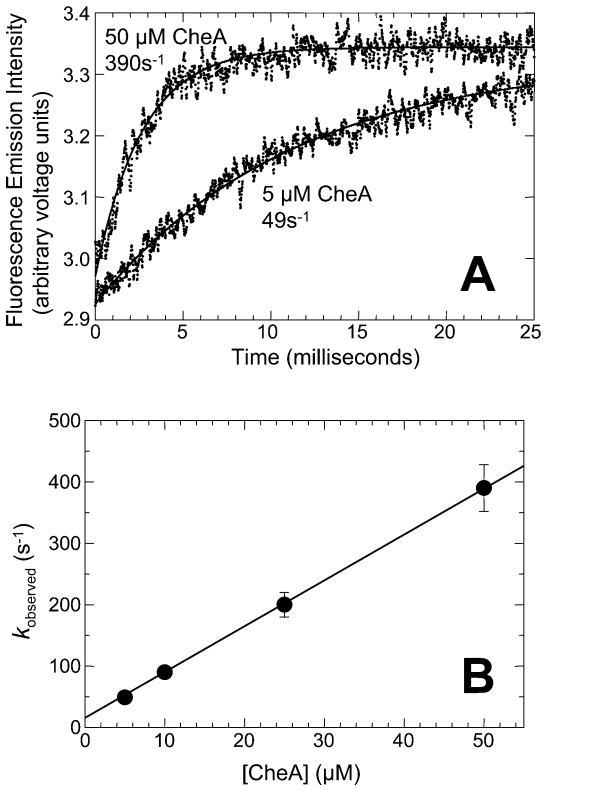


FIGURE 9: Kinetics of CheA binding to Badan-CheY. Fluorescence stopped-flow experiments were performed to monitor the time course of binding after rapid mixing of 1 $\mu$M Badan-CheY with excess full-length wild-type CheA in TNGKGD buffer at 4 °C. (A) Time courses observed for 5 and 50 $\mu$M CheA (concentrations after mixing). Averaged time courses (reflecting 10 records with 2000 time points each) were fit to a single-exponential equation (solid lines indicate the best fits assigned by computer least-squares analysis). This analysis defined the values of pseudo-first-order rate constants ($k_{observed}$). (B) Effect of CheA concentration on the $k_{observed}$ value. The data were fit by linear regression and indicated a *y*-axis intercept of 15 $s^{-1}$ and a slope of 7.5 $\mu M^{-1}$ $s^{-1}$.

any $CheA^{156-229}$, and a higher apparent $K_d$ (6.5 ± 0.3 $\mu$M) was observed in the presence of 4.5 $\mu$M $CheA^{156-229}$. These results suggest that although P2 ($CheA^{156-229}$) does not induce a fluorescence increase in Badan-CheY, it does readily compete with the P1−P2 fragment ($CheA^{1-233}$). Binding of $CheA^{156-229}$ to Badan-CheY could also be inferred from the small decrease in emission signal observed in Figure 8A.

Similar titration experiments, in which Badan-CheY was titrated with full-length CheA, indicated a $K_d$ of 1.7 ± 0.2 $\mu$M for the complex. This value compares favorably with that determined previously under similar conditions by ITC [$K_d$ = 2 ± 0.5 $\mu$M] (*26*) and by fluorescence-monitored titration of CheY with nonfluorescent CheA ($CheA^{W565F}$) [$K_d$ = 1.5 ± 0.8 $\mu$M] (*38*). This agreement indicates that the $Met^{17} \rightarrow Cys$ mutation and covalent attachment of the Badan fluorophore do not significantly affect the CheY−CheA binding equilibrium.

We took advantage of the large emission change of Badan-CheY upon binding to CheA as a way to investigate the kinetics of Badan-CheY binding to full-length CheA. Using stopped-flow fluorescence experiments, we monitored the increase in emission signal after rapid mixing of Badan-CheY with excess CheA (Figure 9A). Each time course generated in these experiments was fit to a single-exponential equation to define the value of the observed pseudo-first-order rate constant ($k_{obs}$). The dependence of $k_{obs}$ on the CheA concentration (Figure 9B) indicated a linear relationship with a nonzero *y*-axis intercept. The simplest reaction scheme consistent with these results is a one-step reversible binding equilibrium:

$$\text{CheY} + \text{CheA} \underset{k_{dissn}}{\overset{k_{assn}}{\rightleftharpoons}} \text{CheY:CheA} \qquad (1)$$

For such a scenario, the slope of Figure 9B would indicate $k_{assn}$ (~7.5 $\mu M^{-1}$ $s^{-1}$), and the *y*-axis intercept would equal $k_{dissn}$ (~15 $s^{-1}$). These values are similar to the $k_{assn}$ (8 $\mu M^{-1}$ $s^{-1}$) and $k_{dissn}$ (20 $s^{-1}$) values we determined previously under very similar conditions ($\mu$ ~ 0.1 M, $T$ = 4 °C; 10% glycerol) by monitoring the fluorescence decrease of CheY $Trp^{58}$ (*38*; R.C.S., unpublished). These previous experiments required use of a version of CheA ($CheA^{W565F}$) engineered to remove its intrinsic fluorescence, an approach that was only partially successful in that the $CheA^{W565F}$ retained enough residual intrinsic fluorescence that made it impossible for us to use CheA concentrations higher than ~20 $\mu$M without increasing the background fluorescence to unmanageable levels. Using

Badan-CheY in the experiments described here, we were able to extend the concentration range out to 100 $\mu$M CheA. No evidence of saturation kinetics was observed at the higher CheA levels, providing further support that the simple one-step equilibrium (eq 1) accurately describes the binding reaction.

## DISCUSSION

We have generated and characterized a fluorescently labeled derivative of CheY that allows simple and sensitive assays to monitor CheY phosphorylation and CheY binding to its cognate kinase, CheA. Similar assays are possible by use of wild-type CheY and monitoring quenching of its intrinsic fluorescence upon phosphorylation and binding to CheA, but the Badan-labeled protein provides several notable advantages. One advantage is sensitivity: the fluorescence emission intensity of the (dimethylamino)naphthalene label of Badan-CheY is much greater than that of $Trp^{58}$ of CheY. Moreover, the absolute changes in emission intensity upon phosphorylation or binding of the protein to CheA are considerably greater for Badan-CheY than for unmodified CheY. Experiments can be carried out easily with Badan-CheY in the 0.1−0.2 $\mu$M range, while similar experiments with wild-type CheY require 10−20 times this concentration to generate data with a comparable signal-to-noise ratio. For some experiments, this can be an important advantage. A second advantage is that the fluorophore of Badan-CheY absorbs and emits light at wavelengths where the absorbance and emission properties of other proteins (such as CheA) and/or other additions (such as ATP) do not interfere. This enables experiments not possible with CheY intrinsic fluorescence as the signal, such as titrations of CheY with full-length versions of CheA. Yet another advantage is that Badan-CheY may provide an opportunity to visualize/monitor CheY interactions with the P1 domain of CheA, something not possible with wild-type CheY. We will consider this point in greater detail below.

Badan-CheY faithfully reproduces many of the properties of wild-type CheY that have been established in previous work: it binds to CheA with the same affinity as does wild-type CheY, and the kinetics of this binding and of phosphotransfer from P-CheA to CheY are indistinguishable from those observed with wild-type CheY. The kinetics of autophosphorylation with small-molecule phosphodonors are also faithfully reproduced with the Badan-labeled protein. Taken together, these results indicate that, with respect to phosphorylation and interactions with CheA, Badan-CheY behaves indistinguishably from wild-type CheY. Dephosphorylation of Badan-CheY, however, differs from that of wild-type CheY: the autodephosphorylation kinetics are somewhat slower with Badan-CheY than with the wild-type protein. This defect was also observed with unlabeled $CheY^{M17C}$ and may indicate a subtle change in the orientation of the active-site groups that mediate dephosphorylation. Our results further indicate that modifications at the $Met^{17}$ position affect the ability of CheY to interact with CheZ: CheZ-catalyzed dephosphorylation was less effective with $CheY^{M17C}$ and was essentially eliminated with the Badan-labeled protein. These results are not surprising in view of the participation of the $Met^{17}$ side chain in binding contacts with CheZ (*64*). In the crystal structure of the complex formed by CheZ and $CheY-BeF_3^- - Mg^{2+}$, CheY makes binding contacts with two distinct regions of CheZ: a long four-helix bundle ($CheZ_{core}$) that contributes a catalytic group ($Gln^{147}$) for dephosphorylation and a 13-amino acid helix that corresponds to the C-terminal end of CheZ. The $Met^{17}$ side chain of CheY interacts with $Asp^{143}$ in the $CheZ_{core}$ region. Therefore, $CheY^{M17C}$ might be expected to exhibit weakened affinity for CheZ, and the bulky Badan fluorophore could prevent CheY−CheZ binding by obstructing other components of the CheY−CheZ binding interface or by preventing/altering access of the CheZ catalytic group to phospho-$Asp^{57}$ of CheY.

The contributions of $Met^{17}$ to CheY function were also investigated in recent work from the Bourret laboratory. In a survey of a large number of CheY point mutants, Smith et al. (*45*) found that replacing $Met^{17}$ with Arg, Asp, Glu, His, Ser, Lys, Thr, or Gln rendered CheY incapable of promoting CW flagellar rotation in vivo (the $Met^{17} \rightarrow$ Cys mutant was not examined); cells expressing such mutant variants of CheY in place of wild-type CheY were nonchemotactic. We found that *E. coli* expressing $CheY^{M17C}$ exhibited similar properties (a $Che^-$ phenotype and extreme counterclockwise flagellar rotation bias), although partial restoration of chemotaxis abilty and clockwise rotation (tumbling) could be achieved by overproduction of the mutant protein (R.C.S., unpublished observations). As noted by Smith et al. (*45*), the "functional intolerance to replacement" at position 17 of CheY could arise from several possible defects in the mutant proteins: (i) diminished ability to become phosphorylated by CheA, (ii) enhanced ability to become dephosphorylated by CheZ, or (iii) defective interactions with the flagellar motor. Our results indicate that, at least for $CheY^{M17C}$, the first two possibilities are not the case, suggesting that the chemotaxis defects of cells expressing $CheY^{M17C}$ arise from diminished ability of the mutant CheY to interact with the flagellar motor. Further work would be required to determine whether this reflects poor binding of $CheY^{M17C}$ to the switch component (FliM) of the motor or decreased ability of $CheY^{M17C}$ to propagate phosphorylation-induced conformational changes to the motor.

Despite some differences from wild-type CheY (as detailed above), Badan-CheY could serve as a useful tool for several kinds of in vitro experiments, in particular those that do not require CheY interactions with CheZ or the flagellar motor. For example, experiments attempting to reconstitute regulation of CheY phosphorylation levels via receptor-mediated control of CheA autokinase activity require simultaneous use of numerous proteins (receptors, CheA, CheW, CheY, and perhaps CheB), each with intrinsic fluorescence signals that make it difficult to monitor CheY phosphorylation status by relying on CheY $Trp^{58}$ fluorescence. By contrast, Badan-CheY generates an unambiguous emission signal at relatively long wavelengths, free of interference from other proteins.

In addition, future work may be able to exploit the nature of the protein−protein interactions underlying the fluorescence change caused by CheA binding to Badan-CheY. Our findings suggest that the increase in emission intensity of the labeled protein is caused by the P1 domain of CheA: a CheA fragment ($CheA^{1-233}$) spanning P1 and P2 generates the same emission increase observed with full-length CheA, while an isolated P2 domain does not cause this spectral change, although it does readily bind to the labeled CheY. Addition of an isolated P1 domain to the P2−Badan-CheY

complex did not generate any significant fluorescence change (results not shown). There are several possible mechanisms by which P1 might affect the emission properties of the Badan label in the context of the complexes formed when Badan-CheY binds to full-length CheA or the P1−P2 fragment: (i) P1 might interact with CheY in a manner that alters the environment of the Badan; (ii) P1 might interact directly with the Badan molecule, independent of any participation of P1−CheY interactions; or (iii) P1 might alter the conformation of P2 in a manner that affects the local environment of Badan. Our results, considered in conjunction with previous studies of CheA structure and dynamics, support the first of these three possibilities. Mechanism iii seems unlikely in view of the NMR results from the Dahlquist research group indicating that P1 and P2 operate as independent (noninteracting) domains connected by a flexible, unstructured linker (*27*). To explore the second possibility (direct P1−Badan interaction), we titrated an isolated P1 domain ($CheA^{1-139}$) into a solution containing a Badan−mercaptoethanol adduct and into a solution of Badan-CheY. In both cases there was no detectable change in the Badan emission spectrum. These results do not support the hypothesis that P1 can interact directly with Badan. However, we cannot completely rule out this possibility because the highest P1 concentration we reached with $CheA^{1-139}$ (100 $\mu$M) is likely to be lower than the effective local concentration of P1 experienced by Badan when Badan-CheY binds to P2 in the context of full-length CheA or $CheA^{1-233}$ (because of the physical tethering of P1 to P2). So the possibility remains that P1 interacts directly with Badan at higher P1 concentrations. However, it should be emphasized that the affinity of Badan-CheY for CheA, the kinetics of the binding reaction, and the kinetics of phosphotransfer from P-CheA to Badan-CheY are essentially identical to those measured previously for interaction of wild-type CheY with CheA (*38*, *39*). This agreement indicates that if, in fact, P1 can interact directly with Badan, this interaction must be quite weak relative to the CheY−P2 binding interaction and must have little or no effect on the ability of P1 to interact with CheY during CheA−CheY phosphotransfer.

We are continuing to explore the P1-dependent fluorescence change in the CheA−Badan-CheY complex as a possible tool to visualize P1−CheY interactions. Such a tool might be useful for assessing whether specific mutations in CheY or P1 alter or eliminate the interaction, information that cannot be acquired from CheY intrinsic fluorescence ($Trp^{58}$). We also note that CheY proteins in the chemotaxis systems of bacteria other than *E. coli* and *S. typhimurium* do not have a tryptophan conveniently located at the active site and so, in these systems, CheY binding and phosphorylation studies cannot make use of sensitive and powerful fluorescence-based experiments. Perhaps such approaches can be applied to these systems after labeling of their CheY proteins with Badan (or other environmentally sensitive fluorophores) attached to cysteine side chains introduced (via site-directed mutagenesis) at positions corresponding to $Met^{17}$ in *E. coli* CheY. We are currently exploring this possibility using CheY from *Thermotoga maritima*.

## ACKNOWLEDGMENT

We thank Sandy Parkinson for numerous *E. coli* strains, Amy Roth for plasmids, and Anna Kolesar for comments on the manuscript. We also gratefully acknowledge constructive criticism from one of the anonymous reviewers leading to improvements in Figure 1.

## REFERENCES

1. Armitage, J. P. (1999) Bacterial tactic responses, *Adv. Microb. Physiol. 41*, 229−289.
2. Berg, H. C., and Brown, D. A. (1972) Chemotaxis in *Escherichia coli* analyzed by three-dimensional tracking, *Nature 239*, 500−504.
3. Macnab, R. M. (1996) in *Escherichia coli and Salmonella typhimurium: Cellular and Molecular Biology* (Neidhardt, F. C., Ed.) pp 123−145, ASM Press, Washington, DC.
4. Dahlquist, F. W., Lovely, P., and Koshland, D. E., Jr. (1972) Quantitative analysis of bacterial migration in chemotaxis, *Nature 236*, 120−123.
5. Weiss, R. M., and Koshland, D. E., Jr. (1990) Chemotaxis in *Escherichia coli* proceeds efficiently from different initial tumble frequencies, *J. Bacteriol. 172*, 1099−1105.
6. Khan, S., Castellano, F., Spudich, J. L., McCray, J. A., Goody, R. S., Reid, G. P., and Trentham, D. R. (1993) Excitatory signaling in bacteria probed by caged chemoeffectors, *Biophys. J. 65*, 2368−2382.
7. Block, S. M., Segall, J. E., and Berg, H. C. (1982) Impulse responses in bacterial chemotaxis, *Cell 32*, 215−226.
8. Sourjik, V., and Berg, H. C. (2002) Binding of the *Escherichia coli* response regulator CheY to its target measured in vivo by fluorescence resonance energy transfer, *Proc. Natl. Acad. Sci. U.S.A. 99*, 12669−12674.
9. Welch, M., Oosawa, K., Aizawa, S.-I., and Eisenbach, M. (1994) Effects of phosphorylation, $Mg^{2+}$, and conformation of the chemotaxis protein CheY on its binding to the flagellar switch protein FliM, *Biochemistry 33*, 10470−10476.
10. Welch, M., Oosawa, K., Aizawa, S.-I., and Eisenbach, M. (1993) Phosphorylation-dependent binding of a signal molecule to the flagellar switch of bacteria, *Proc. Natl. Acad. Sci. U.S.A. 90*, 8787−8791.
11. Hess, J. F., Oosawa, K., Kaplan, N., and Simon, M. I. (1988) Phosphorylation of three proteins in the signaling pathway of bacterial chemotaxis, *Cell 53*, 79−87.
12. Hess, J. F., Bourret, R. B., Oosawa, K., Matsumura, P., and Simon, M. I. (1988) Protein phosphorylation and bacterial chemotaxis, *Cold Spring Harbor Symp. Quant. Biol. 53*, 41−48.
13. Borkovich, K. A., Kaplan, N., Hess, J. F., and Simon, M. I. (1989) Transmembrane signal transduction in bacterial chemotaxis involves ligand-dependent activation of phosphate group transfer, *Proc. Natl. Acad. Sci. U.S.A. 86*, 1208−1212.
14. Borkovich, K. A., and Simon, M. I. (1990) The dynamics of protein phosphorylation in bacterial chemotaxis, *Cell 63*, 1339−1348.
15. Gegner, J. A., Graham, D. R., Roth, A. F., and Dahlquist, F. W. (1992) Assembly of an MCP receptor, CheW, and kinase CheA complex in the bacterial chemotaxis signal transduction pathway, *Cell 18*, 975−982.
16. Liu, U., Levit, M., Lurz, R., Surette, M. G., and Stock, J. B. (1997) Receptor-mediated protein kinase activation and the mechanism of transmembrane signaling in bacterial chemotaxis, *EMBO J. 16*, 7231−7240.
17. Levit, M., Liu, Y., and Stock, J. B. (1999) Mechanism of CheA protein kinase activation in receptor signaling complexes, *Biochemistry 38*, 6651−6658.
18. Francis, N. R., Levit, M. N., Shaikh, T. R., Melanson, L. A., Stock, J. B., and DeRosier, D. J. (2002) Subunit organization in a soluble complex of Tar, CheW, and CheA by electron microscopy, *J. Biol. Chem. 277*, 36755−36759.
19. West, A. H., and Stock, A. M. (2001) Histidine kinases and response regulator proteins in two-component signaling systems, *Trends Biochem. Sci. 26*, 369−376.
20. Stock, A. M., Mottonen, J., Stock, J. B., and Schutt, C. E. (1989) Three-dimensional structure of CheY, the response regulator of bacterial chemotaxis, *Nature 337*, 745−749.
21. Stock, A. M., Martinez-Hackert, E., Rasmussen, F. B., West, A. H., Stock, J. B., Ringe, D., and Petsko, G. A. (1993) Structure of the Mg(+2) bound form of CheY and mechanism of phosphoryl transfer in bacterial chemotaxis, *Biochemistry 32*, 13376−13380.
22. Sanders, D. A., Gillece-Castro, Stock, A. M., B. L., Burlingame, A. L., and Koshland, D. E., Jr. (1992) Identification of the site of

phosphorylation of the chemotaxis response regulator CheY, *J. Biol. Chem. 264*, 21770−21778.
23. Lukat, G. S., McCleary, W. R., Stock, A. M., and Stock, J. B. (1992) Phosphorylation of bacterial response regulator proteins by low molecular weight phospho-donors, *Proc. Natl. Acad. Sci. U.S.A. 89*, 718−722.
24. Silversmith, R. E., Appleby, J. L., and Bourret, R. B. (1997) Catalytic mechanism of phosphorylation and dephosphorylation of CheY: kinetic characterization of imidazole phosphates as phosphodonors and the role of acid catalysis, *Biochemisry 36*, 14965−14974.
25. Hess, J. F., Bourret, R. B., and Simon, M. I. (1988) Histidine phosphorylation and phosphoryl group transfer in bacterial chemotaxis, *Nature 336*, 139−143.
26. Li, J., Swanson, R. V., Simon, M. I., and Weis, R. M. (1995) The response regulators CheB and CheY exhibit competitive binding to the kinase CheA, *Biochemistry 34*, 14626−1463.
27. Zhou, H. J., McEvoy, M. M., Lowry, D. F., Swanson, R. V., Simon M. I., Dahlquist. F. W. (1996) Phosphotransfer and CheY-binding domains of the histidine autokinase CheA are joined by a flexible linker, *Biochemistry 35*, 433−443.
28. Stewart, R. C., Jahreis, K., and Parkinson, J. S. (2000) Rapid phosphotransfer to CheY from a CheA protein lacking the CheY-binding domain, *Biochemistry 39*, 13157−13165.
29. Bilwes, A., Alex., L., Crane, B. R., and Simon, M. I. (1999) Structure of CheA, a signal-transducing histidine kinase, *Cell 96*, 131−141.
30. Surette, M. L., M., Liu, Y., Lukat, G., Ninfa, E., Ninfa, A., and Stock, J. (1996) Dimerization is required for the activity of the protein histidine kinase CheA that mediates signal transductin in bacterial chemotaxis, *J. Biol. Chem. 271*, 939−945.
31. Bilwes, A., Quezada, C. M., Croal, L. R., Crane, B. R., and Simon, M. I. (2001) Nucleotide binding by the histidine kinase CheA, *Nat. Struct. Biol. 8*, 353−360.
32. Bourret, R. B., Davagnino, J., and Simon, M. I. (1993) The carboxy-terminal portion of the CheA kinase mediates regulation of autophosphorylation by transducer and CheW, *J. Bacteriol. 175*, 2097−2101.
33. McEvoy, M. M., Zhou, J., Roth, A. F., Lowry, D. F., Morrison, T. B., Kay, L. E., and Dahlquist, F. W. (1995) Nuclear magnetic resonance assignments and global fold of a CheY-binding domain in CheA, the chemotaxis-specific kinase of *Escherichia coli*, *Biochemistry 34*, 13871−13880.
34. McEvoy, M. M., Muhandiram, D. R., Kay, L. E., and Dahlquist, F. W. (1996) Structure and dynamics of a CheY-binding domain of the chemotaxis kinase CheA determined by nuclear magnetic resonance spectroscopy, *Biochemistry 35*, 5633−5640.
35. Swanson, R. V., Lowry, D. F., Matsumura, P., McEvoy, M. M., Simon, M. I., and Dahlquist, F. W. (1995) Localized perturbations in CheY structure monitored by NMR identify a CheA binding interface, *Nat. Struct. Biol. 2*, 906−910.
36. McEvoy, M. M., Bren, A., Eisenbach, M., and Dahlquist, F. W. (1999) Identification of the binding interfaces on CheY for two of its targets, the phosphatase CheZ and the flagellar switch protein FliM, *J. Mol. Biol. 289*, 1423−1433.
37. Shukla, D., and Matsumura, P. (1995) Mutations leading to altered CheA binding cluster on a face of CheY, *J. Biol. Chem. 270*, 24414−24419.
38. Stewart, R. C., and Van Bruggen, R. (2004) Association and dissociation kinetics for CheY interacting with the P2 domain of CheA, *J. Mol. Biol. 336*, 287−301.
39. Mayover, T. C., Halkides, C. J., and Stewart, R. C. (1999) Kinetic characterization of CheY phosphorylation reactions: comparison of P-CheA and small-molecule phosphodonors, *Biochemistry 38*, 2259−2271.
40. Da Re, S. S., Deville-Bonne, D., Tolstykh, T., Veron, M., and Stock, J. B. (1999) Kinetics of CheY phosphorylation by small molecule phosphodonors, *FEBS Lett. 457*, 323−326.
41. Smith, J. G., Latiolais, J. A., Guanga, G. P., Pennington, J. D., Silversmith, R. E., and Bourret, R. B. (2004) A search for amino acid substitutions that universally activate response regulators, *Mol. Microbiol. 51*, 887−901.
42. Kunkel, T. A., Roberts, J. D., and Zakour, R. (1987) Rapid and efficient site-specific mutagenesis without phenotypic selection, *Methods Enzymol. 154*, 367−382.
43. Wolfe, A. J., and Stewart, R. C. (1993) The short form of the CheA protein restores kinase activity an chemotactic ability to kinase-deficient mutants, *Proc. Natl. Acad. Sci. U.S.A. 90*, 1518−1522.
44. Wolfe, A. J., and Berg., H. C. (1989) Migration of bacteria in semisolid agar, *Proc. Natl. Acad. Sci. U.S.A. 86*, 6973−6977.
45. Smith, J. G., Latiolais, J. A., Guanga, G. P., Citineni, S., Silversmith, R. E., and Bourret, R. B. (2003) Investigation of the role of electrostatic charge in activation of the *Escherichia coli* response regulator CheY, *J. Bacteriol. 185*, 6385−6391.
46. Gegner, J., and Dahlquist, F. W. (1991) Signal transduction in bacteria: CheW forms a reversible complex with the protein kinase CheA, *Proc. Natl. Acad. Sci. U.S.A. 88*, 750−754.
47. Muchmore, D. C., McIntosh, L. P., Ruseell, C. B., Anderson, D. E., and Dahlquist, F. W. (1989) *Methods Enzymol. 177*, 44−73.
48. Liu, J., and Parkinson, J. S. (1989) Role of CheW protein in coupling membrane receptors to the intracellular signaling system of bacterial chemotaxis, *Proc. Natl. Acad. Sci. U.S.A. 86*, 8703−8707.
49. Studier, F. W., Rosenberf, A. H., Dunn, J. J., and Dubendorff, J. W. (1990) Use of T7 RNA-polymerase to direct expression of cloned genes, *Methods. Enzymol. 185*, 60−89.
50. Levit, M., Liu, Y., Surette, M., and Stock, J. (1996) Active site interference and asymmetric activation in the chemotaxis protein histidine kinase CheA, *J. Biol. Chem. 271*, 32057−32063.
51. Stock, A., Koshland, D. E., Jr., and Stock, J. (1985) Homologies between the Salmonella-typhimurium CheY protein and proteins involved in the regulation of chemotaxis, membrane-protein synthesis, and sporulation, *Proc. Natl. Acad. Sci. U.S.A. 82*, 7989−7993.
52. Stewart, R. C., VanBruggen, R., Ellefson, D. D., and Wolfe, A. J. (1998) TNP-ATP and TNP-ADP as probes of the nucleotide binding site of CheA, the histidine protein kinase in the chemotaxis signal transduction pathway of *Escherichia coli*, *Biochemistry 37*, 12269−12279.
53. Gill, S., and von Hippel, P. H. (1989) Calculation of protein extinction coefficients from amino acid sequence data, *Anal. Biochem. 182*, 319−326.
54. Hirschman, A., Boukhvalova, M., VanBruggen, R., Wolfe, A. J., and Stewart, R. C. (2001) Active site mutations in CheA, the signal-transducing protein kinase of the chemotaxis system in *Escherichia coli*, *Biochemistry 40*, 13876−13887.
55. Boxrud, P. D., Fay, W. P., and Bock, P. E. (2000) Streptokinase binds to human plasmin with high affinity, perturbs the plasmin active site, and induces expression of a substrate recognition exosite for plasminogen, *J. Biol. Chem. 275*, 14579−14589.
56. Kuzmic, P. (1996) Program DYNAFIT for the analysis of enzyme kinetic data: application to HIV proteinase, *Anal. Biochem. 237*, 260−273.
57. Brissette, P., Ballou, D. P., and Massey, V. (1989) Determination of the dead time of a stopped-flow fluorometer, *Anal. Biochem. 181*, 234−238.
58. Lowry, D. F., Roth, A. F., Rupert, P. B., Dahlquist, F. W., Moy, F. J., Domaille, P. J., and Matsumura, P. (1994) Signal transduction in chemotaxis. A propagating conformational change upon phosphorylation of CheY, *J. Biol. Chem. 269*, 26358−26362.
59. Cho, H. S., Lee, S.-Y., Yan, D., Pan, X., Parkinson, J. S., Kustu, S., Wemmer, D. S., and Pelton, J. G. (2000) NMR structure of activated CheY, *J. Mol. Biol 297*, 543−551.
60. Lee, S.-Y., Cho, H. S., Pelton, J. G., Yan, D., Berry, E. A., and Wemmer, D. E. (2001) Crystal structure of activated CheY: comparison with other activated receiver domains, *J. Biol. Chem. 276*, 16425−16431.
61. McEvoy, M. M., Hausrath, A. C., Randolph, G. B., Remington, S. J., and Dahlquist, F. W. (1998) Two binding modes reveal flexibility in kinase/response regulator interactions in the bacterial chemotaxis pathway, *Proc. Natl. Acad. Sci. U.S.A. 95*, 7333−7338.
62. Welch, M. C., N., Mourey, L., Birck, C., and Samama, J.-P. (1997) Structure of the CheY-binding domain of histidine kinase CheA in complex with CheY, *Nat. Struct. Biol. 5*, 25−29.
63. Lee, S.-Y., Cho, H. S., Pelton, J. G., Yan, D., Henderson, R. K., King, D. S., Huang, L.-S., Kustu, S., Berry, E. A., and Wemmer, D. E. (2001) Crystal structure of an activated response regulator bound to its target, *Nat. Struct. Biol. 8*, 52−56.
64. Zhao, R., Collins, E. J., Bourret, R. B., and Silversmith, R. E. (2002) Structure and catalytic mechanism of the *E. coli* chemotaxis phosphatase CheZ, *Nat. Struct. Biol. 9*, 570−575.
65. Lukat, G. S., Stock, A. M., and Stock, J. B. (1990) Divalent metal ion binding to the CheY protein and its significance to phosphotransfer in bacterial chemotaxis, *Biochemistry 29*, 5436−5442.
66. Yan, D., Cho, H. S., Hastings, C. A., Igo, M. M., Lee, S.-Y., Pelton, J. G., Stewart, V., Wemmer, D. E., and Kustu, S. (1999) Beryllofluoride mimics phosphorylation of NtrC and other bacte-

rial response regulators, *Proc. Natl. Acad. Sci. U.S.A. 96*, 14789−14794.
67. Simonovic, M., and Volz, K. (2001) A distinct meta-active conformatin in the 1.1 Å resolution structure of wild-type apoCheY, *J. Biol. Chem. 276*, 28637−28640.
68. Guex, N., and Peitsch, M. C. (1997) SWISS-MODEL and the Swiss-Pdb Viewer: An environment for comparative protein modeling, *Electrophoresis 18*, 2714−2723.
69. Morrison, T. B., and Parkinson, J. S. (1994) Liberation of an interaction domain from the phosphotransfer region of CheA, a signaling kinase of *Escherichia coli*, *Proc. Natl. Acad. Sci. U.S.A. 91*, 5485−5489.
70. Swanson, R. V., Schuster, S. C., and Simon, M. I. (1993) Expression of CheA fragments which define domains encoding kinase, phosphotransfer, and CheY binding activities, *Biochemistry 32*, 7623−7629.
71. Morrison, T. B., and Parkinson, J. S. (1997) A fragment liberated from the *E. coli* kinase that blocks stimulatory, but not inhibitory, chemoreceptor signaling, *J. Bacteriol. 179*, 5543−5550.
72. Schuster, M., Zhao, R., Bourret, R. B., and Collins, E. J. (2000) Correlated switch binding and signaling in bacterial chemotaxis, *J. Biol. Chem. 275*, 19752−19758.

BI0495735